the charging voltage of the main condenser, and the maximum tube current was approximately 15 kA.

3.2 X-ray output

X-ray output pulse was detected using a combination of a plastic scintillator and a photomultiplier using a 10 μm-thick monochromatic copper filter (Fig. 5). The x-ray pulse height substantially increased with corresponding increases in the charging voltage. The x-ray pulse widths were about 700 ns, and the time-integrated x-ray intensity per pulse measured by a thermoluminescence dosimeter (Kyokko TLD Reader 1500 utilizing MSO-S elements without energy compensation) had a value of about 30 μC/kg at 1.0 m from the x-ray source with a charging voltage of 50 kV.

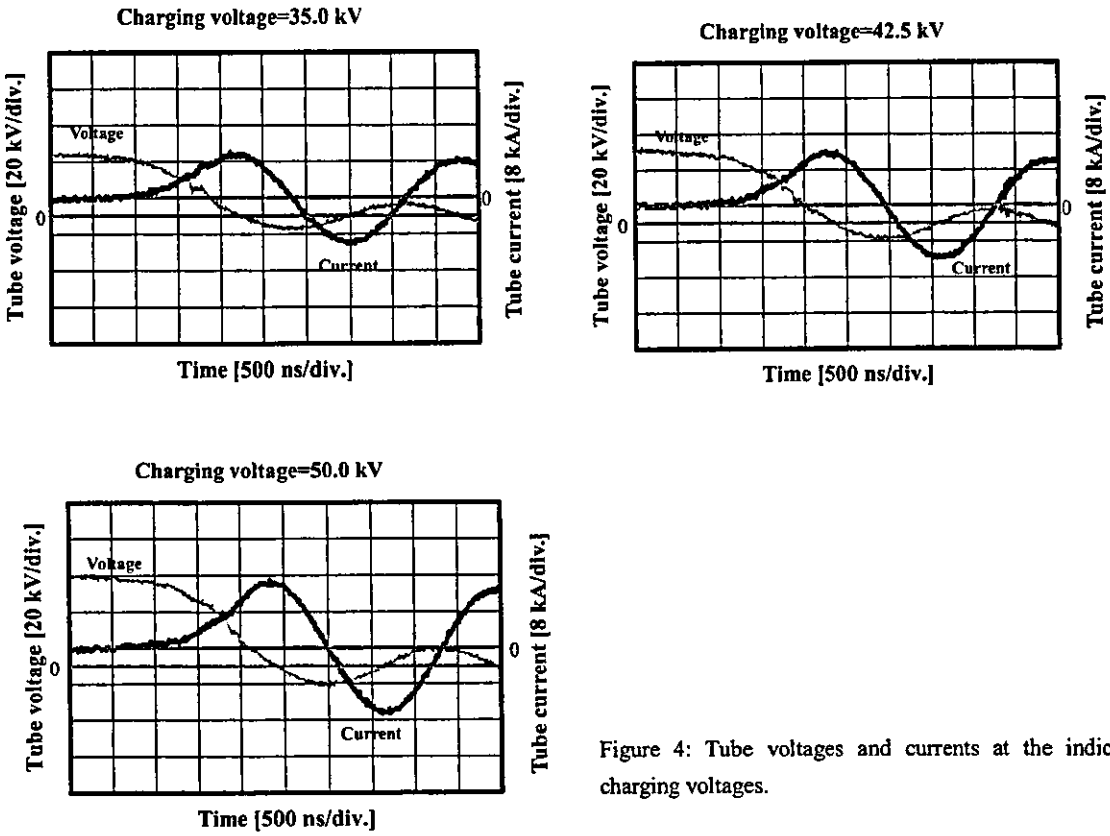

Figure 4: Tube voltages and currents at the indicated charging voltages.

3.3 X-ray source

In order to measure images of the plasma x-ray source, we employed a pinhole camera with a hole diameter of 100 μm (Fig. 6). When the charging voltage was increased, the plasma x-ray source grew, and both spot dimension and intensity increased.

3.4 X-ray spectra

X-ray spectra from the plasma source were measured by a transmission-type spectrometer (Fig. 7) with a lithium

fluoride curved crystal 0.5 mm in thickness. The spectra were taken by a computed radiography (CR) system[22] (Konica Regius 150) with a wide dynamic range, using the filter, and relative x-ray intensity was calculated from Dicom digital data. Figure 8 shows measured spectra from the copper target using the filter. In fact, we observed sharp lines of K-series characteristic x-rays such as lasers, while bremsstrahlung rays were hardly detected at all. The characteristic x-ray intensity of the K_α line substantially increased with corresponding increases in the charging voltage, and the K_β line was absorbed by the filter.

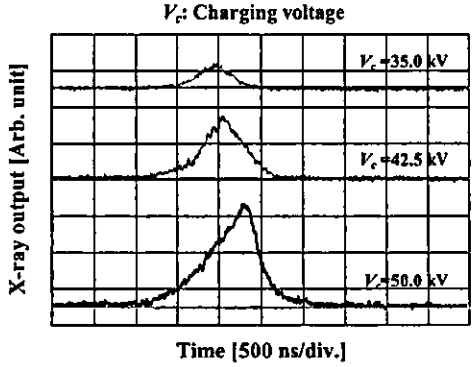

Figure 5: X-ray outputs measured by a plastic scintillator with changes in the charging voltage.

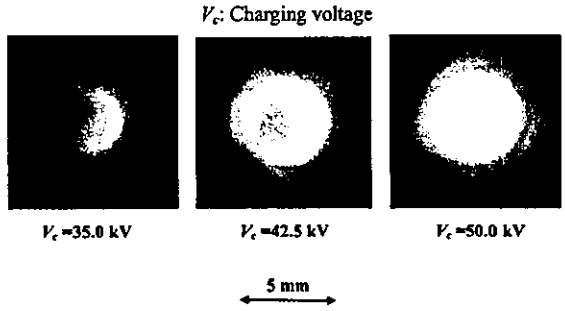

Figure 6: Images of the plasma x-ray source measured by a pinhole of 100 μm from the plasma axial direction.

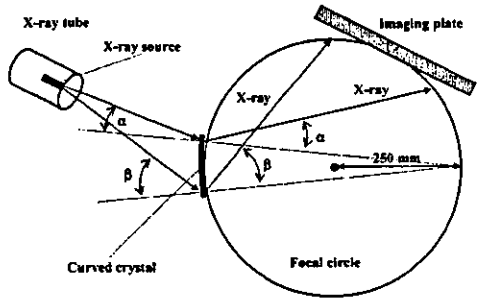

Figure 7: Transmission-type spectrometer with a lithium fluoride curved crystal and an imaging plate.

3.5 X-ray divergence by slits

In order to ascertain the difference in characteristics between x-rays from a conventional tube and these from the plasma tube, we employed two lead slits in order to measure the divergence of the x-rays (Fig. 9). As compared with incoherent x-rays from a conventional tube with a tungsten target, the characteristic x-rays from the linear plasma were diffused greatly after passing through the two slits (Fig. 10).

3.6 Rectilinear power

Figure 11 shows the experimental setup for measuring the rectilinear power of the K_α lines from a conventional tube and that from the plasma tube using the spectrometer previously described. In this experiment, we measured the coefficient (I_k/I_i) of peak diffraction intensity of K_α (I_k) to transmission intensity (I_i). In the case where the

conventional tube was used, we employed the filter with a tube voltage of 17 kV. When the charging voltage was increased, the linear plasma grew, and the I_k/I_t decreased to approximately 0.004. As compared with a value of 0.009 obtained by the conventional tube, the rectilinear power may be increased, because the values from the plasma were approximately halved.

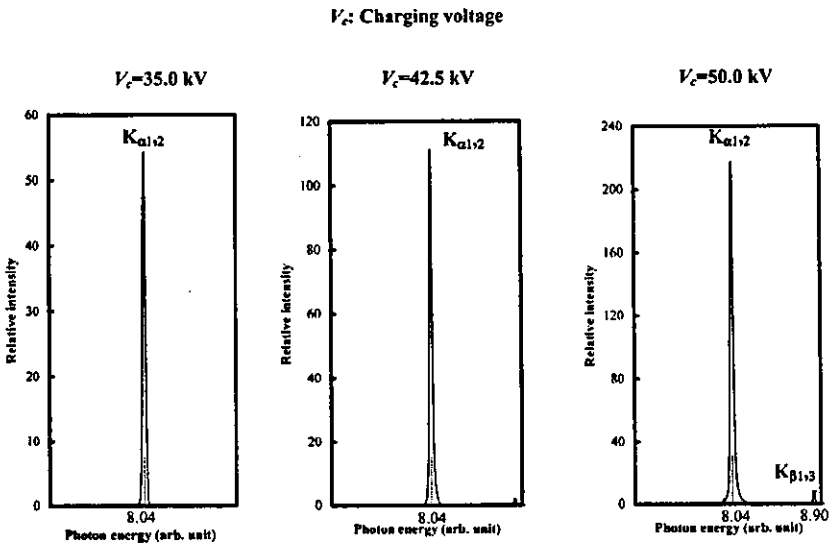

Figure 8: X-ray spectra from weakly ionized copper plasma according to changes in the charging voltage and to insertion of a nickel monochromatic filter.

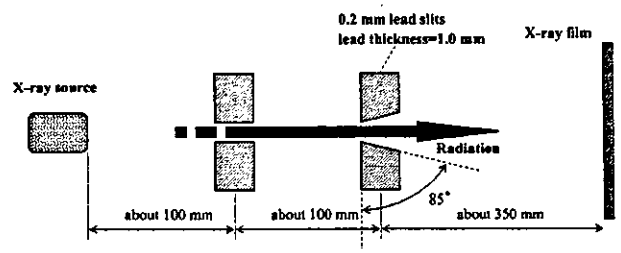

Figure 9: Experimental setup for measuring x-ray divergence using two lead slits.

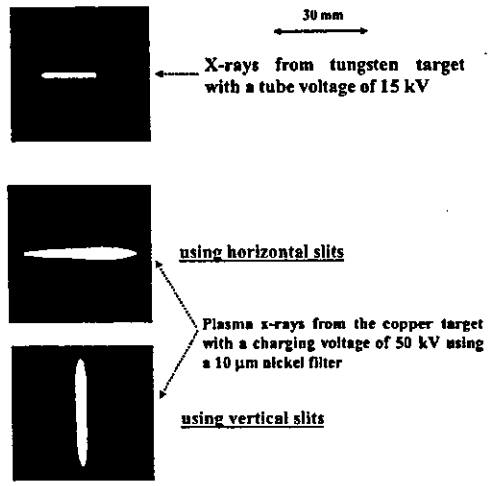

Figure 10: X-ray divergence with two lead slits.

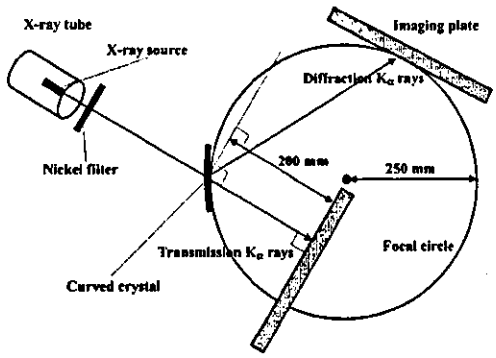

Figure 11: Experimental setup for roughly determining the rectilinear power of the characteristic K_α lines.

4. RADIOGRAPHY

The plasma radiography was performed by the CR system without using the filter, and the distance between the x-ray source and imaging plate was 1.2 m.

Firstly, rough measurements of image resolution were made using wires. Figure 12 shows radiograms of 50 μm-diameter tungsten wires coiled around a pipe and a rod made of polymethyl methacrylate with a charging voltage of 50 kV. Although the image contrast increased using the pipe, 50 μm-diameter wires could be observed.

The image of water falling into a polypropylene beaker from a glass test tube is shown in Fig. 13. This image was taken with a charging voltage of 45 kV, with the slight addition of an iodine-based contrast medium. Because the x-ray duration was about 1 μs, the stop-motion image of water could be obtained.

Figure 14 shows an angiogram of a rabbit heart; iodine-based microspheres of 20 μm in diameter were used with a charging voltage of 50 kV, and fine blood vessels of about 100 μm were visible.

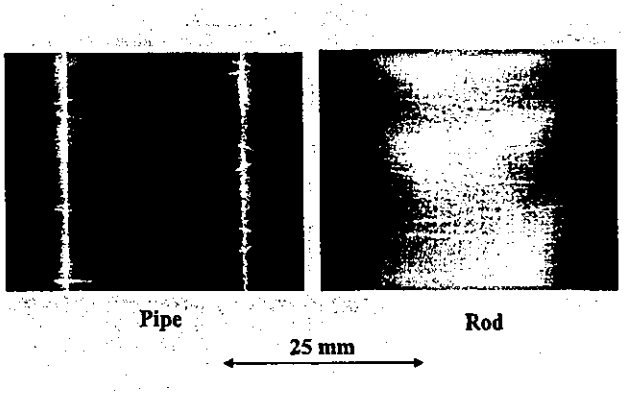

Figure 12: Radiograms of tungsten wires of 50 μm in diameter coiled around a pipe and a rod made of polymethyl methacrylate.

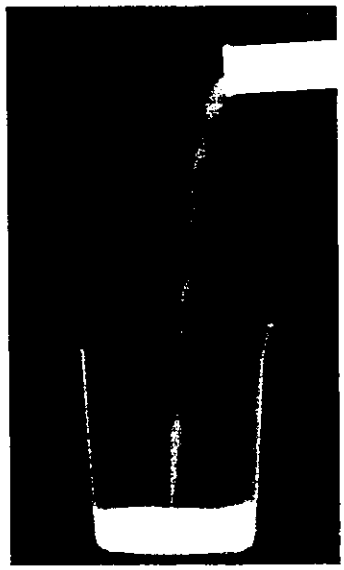

Figure 13: Radiogram of water falling into a polypropylene beaker from a glass test tube.

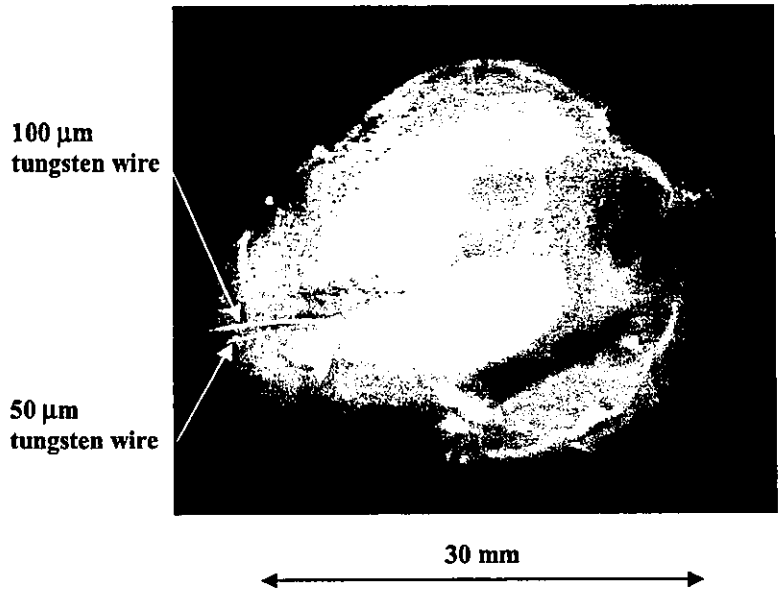

Figure 14: Angiograms of a rabbit heart.

5. DISCUSSION

Concerning the spectrum measurement, we obtained fairly intense and sharp K_α lines from a weakly ionized linear plasma x-ray source by absorbing K_β lines using the monochromatic filter. In fact, these rays were diffused after passing through slits, and this x-ray divergence mechanism has to be solved clearly. Because the diffracting intensity rate decreases with increases in the charging voltage, the rectilinear power may be increased.

In this research, we obtained sufficient characteristic x-ray intensity per pulse for CR radiography using a monochromatic filter, and the generator produced high-count-rate monochromatic photons as compared with the synchrotron monochromatic photons. In addition, since the photon energy of characteristic x-rays can be controlled by changing the target elements, various quasi-monochromatic high-speed radiographies, such as high-contrast micro angiography[23] and parallel radiography[24,25] using an x-ray lens, will be possible.

ACNOWLEDGMENT

This work was supported by Grants-in-Aid for Scientific Research (12670902, 13470154, and 13877114) and Advanced Medical Scientific Research from MECSST, Grants from Keiryo Research Foundation, JST (Test of Fostering Potential), NEDO, and MHLW (HLSRG, RAMT-nano-001, RHGTEFB-genome-005, and RGCD13C-1).

REFERENCES

1. A. Mattsson, "Some characteristics of a 600 kV flash x-ray tube," *Physica Scripta*, **5**, pp. 99-102, 1972.

2. R. Germer, "X-ray flash techniques," *J. Phys. E: Sci. Instrum.*, **12**, pp. 336-350, 1979.

3. C. Cavailler, "AIRIX- a new tool for flash radiography in detonics," *SPIE*, **4183**, pp. 23-35, 2000.

4. E. Sato, H. Isobe and F. Hoshino, "High intensity flash x-ray apparatus for biomedical radiography," *Rev. Sci. Instrum.*, **57**, pp. 1399-1408, 1986.

5. E. Sato, M. Sagae, K. Takahashi, T. Oizumi, H. Ojima, K. Takayama, Y. Tamakawa, T. Yanagisawa, A. Fujiwara and K. Mitoya, "High-speed soft x-ray generators in biomedicine," *SPIE*, **2513**, pp. 649-667, 1994.

6. E. Sato, M. Sagae, K. Takahashi, A. Shikoda, T. Oizumi, H. Ojima, K. Takayama, Y. Tamakawa, T. Yanagisawa, A. Fujiwara and K. Mitoya, "Dual energy flash x-ray generator," *SPIE*, **2513**, pp. 723-735, 1994.

7. E. Sato, M. Sagae, A. Shikoda, K. Takahashi, T. Oizumi, M. Yamamoto, A. Takabe, K. Sakamaki, Y. Hayasi, H. Ojima, K. Takayama and Y. Tamakawa, "High-speed soft x-ray techniques," *SPIE*, **2869**, pp. 937-955, 1996.

8. E. Sato, S. Kimura, S. Kawasaki, H. Isobe, K. Takahashi, Y. Tamakawa and T. Yanagisawa, "Repetitive flash x-ray generator utilizing a simple diode with a new type of energy-selective function," *Rev. Sci. Instrum.*, **61**, pp. 2343-2348, 1990.

9. S. Kimura, E. Sato, M. Sagae, A. Shikoda, T. Oizumi, K. Takahashi, Y. Tamakawa and T. Yanagisawa, "Disk-cathode flash x-ray tube driven by a repetitive two-stage Marx pulser," *Med. & Biol. Eng. & Comput.*, **31**, pp. S37-S43, 1993.

10. A. Shikoda, E. Sato, M. Sagae, T. Oizumi, Y. Tamakawa and T. Yanagisawa, "Repetitive flash x-ray generator having a high-durability diode driven by a two-cable-type line pulser," *Rev. Sci. Instrum.*, **65**, pp. 850-856, 1994.

11. E. Sato, K. Takahashi, M. Sagae, S. Kimura, T. Oizumi, Y. Hayasi, Y. Tamakawa and T. Yanagisawa, "Sub-kilohertz flash x-ray generator utilizing a glass-enclosed cold-cathode triode," *Med. & Biol. Eng. & Comput.*, **32**, pp. 289-294, 1994.

12. K. Takahashi, E. Sato, M. Sagae, T. Oizumi, Y. Tamakawa and T. Yanagisawa, "Fundamental study on a long-duration flash x-ray generator with a surface-discharge triode," *Jpn. J. Appl. Phys.*, **33**, pp. 4146-4151, 1994.

13. J.J. Rocca, V. Shlyaptsev, F.G. Tomasel, O.D.Cortazar, D. Hartshorn and J.L.A. Chilla, "Demonstration of a discharge pumped table-top soft x-ray laser," *Phys. Lev. Lett.*, **73**, pp. 2192-2195, 1994.

14. J.J. Rocca, D.P. Clark, J.L.A. Chilla and V.N. Shlyaptsev, "Energy Extration and achievement of the saturation limit in a discharge-pumped table-top soft x-ray amplifier," *Phys. Lev. Lett.*, **77**, pp. 1476-1479, 1996.

15. C.D. Macchietto, B.R. Benware and J.J. Rocca, "Generation of millijoule-level soft-x-ray laser pulses at a 4-Hz repetition rate in a highly saturated tabletop capillary discharge amplifier," *Opt. Lett.*, **24**, pp. 1115-1117, 1999.

16. J.J.G. Rocca, J.L.A. Chilla, S. Sakadzic, A. Rahman, J. Filevich, E. Jankowska, E.C. Hammarsten, B.M. Luther, H.C. Kapteyn, M. Murnane and V.N. Shlyapsev, "Advances in capillary discharge soft x-ray laser research," *SPIE*, **4505**, pp. 1-6 2001.

17. E. Sato, M. Sagae, T. Ichimaru, Y. Hayasi, H. Ojima, K. Takayama, H. Ido, K. Sakamaki and Y. Tamakawa, "Tentative study on x-ray enhancement by fluorescent emission of radiation by plasma x-ray source," *SPIE*, **3771**, pp. 51-60, 1999.

18. E. Sato, Y. Suzuki, Y. Hayashi, E. Tanaka, H. Mori, T. Kawai, K. Takayama, H. Ido and Y. Tamakawa, "High-intensity quasi-monochromatic x-ray irradiation from the linear plasma target," *SPIE*, **4505**, pp. 154-164, 2001.

19. E. Sato, Y. Hayashi, E. Tanaka, H. Mori, T. Kawai, H. Obara, T. Ichimaru, K. Takayama, H. Ido, T. Usuki, K. Sato and Y. Tamakawa, "Polycapillary radiography using a quasi-x-ray laser generator," *SPIE*, **4508**, pp. 176-187, 2001.

20. E. Sato, Y. Hayasi, E. Tanaka, H. Mori, T. Kawai, T. Usuki, K. Sato, H. Obara, T. Ichimaru, K. Takayama, H. Ido and Y. Tamakawa, "Quasi-monochromatic radiography using a high-intensity quasi-x-ray laser generator," *SPIE*,

4682, pp. 538-548 2002.

21. E. Sato, Y. Hayasi, R. Germer, E. Tanaka, H. Mori, T. Kawai, H. Obara, T. Ichimaru, K. Takayama and H. Ido, "Intense characteristic x-ray irradiation from weakly ionized linear plasma and applications," *Jpn. J. Med. Imag. Inform. Sci.*, **20**, pp. 148-155. 2003.

22. E. Sato , K. Sato and Y. Tamakawa, "Film-less computed radiography system for high-speed Imaging," *Ann. Rep. Iwate Med. Univ. Sch. Lib. Arts and Sci.*, **35**, pp. 13-23, 2000.

Quasi-monochromatic polycapillary imaging utilizing a computed radiography system

Eiichi Sato[a], Yasuomi Hayasi[a], Etsuro Tanaka[b], Hidezo Mori[c], Toshiaki Kawai[d], Toshio Ichimaru[e], Fumiko Obata[f], Kiyomi Takahashi[f], Sigehiro Sato[f], Kazuyoshi Takayama[g] and Hideaki Ido[h]

[a]Department of Physics, Iwate Medical University, 3-16-1 Honchodori, Morioka 020-0015, Japan
[b] Department of Nutritional Science, Faculty of Applied Bio-science, Tokyo University of Agriculture, 1-1-1 Sakuragaoka, Setagaya-ku 156-8502, Japan
[c] Department of Cardiac Physiology, National Cardiovascular Center Research Institute, 5-7-1 Fujishiro-dai, Suita, Osaka 565-8565, Japan
[d] Electron Tube Division #2, Hamamatsu Photonics Inc., 314-5 Shimokanzo, Toyooka Village, Iwata-gun 438-0193, Japan
[e] Department of Radiological Technology, School of Health Sciences, Hirosaki University, 66-1 Honcho, Hirosaki 036-8564, Japan
[f] Department of Microbiology, School of Medicine, Iwate Medical University, 19-1 Uchimaru, Morioka 020-8505, Japan
[g] Shock Wave Research Center, Institute of Fluid Science, Tohoku University, 2-1-1 Katahira, Aoba-ku, Sendai 980-8577, Japan
[h] Department of Applied Physics, Faculty of Engineering, Tohoku Gakuin University, 1-13-1 Chuo, Tagajo 985-8537, Japan

ABSTRACT

A fundamental study on quasi-monochromatic parallel radiography using a polycapillary plate and a copper-target x-ray tube is described. The x-ray generator consists of a negative high-voltage power supply, a filament (hot cathode) power supply, and an x-ray tube. The negative high-voltage is applied to the cathode electrode, and the anode electrode is connected to the ground. In this experiment, the tube voltage was regulated from12 to 22 kV, and the tube current was regulated within 3.0 mA by the filament temperature. The exposure time was controlled in order to obtain optimum x-ray intensity, and the maximum focal spot dimensions were approximately 2.0×1.5 mm. The polycapillary plate was J5022-16 (Hamamatsu Photonics Inc.), and the plate thickness was 1.0 mm. The outer, effective, and hole diameters were 33 mm, 27 mm, and 10 μm, respectively. Quasi-monochromatic x-rays were produced using a 10 μm-thick copper filter with a tube voltage of 17 kV, and these rays were formed into parallel beams by the polycapillary. The radiogram was taken using a computed radiography system utilizing imaging plates. In the measurement of image resolution, the resolution hardly varied according to increases in the distance between the chart and imaging plate using a polycapillary. We could observe a 50 μm tungsten wire clearly, and fine blood vessels of approximately 100 μm were visible in angiography.

Keywords: Parallel radiography, quasi-monochromatic x-ray, characteristic x-ray, x-ray lens, polycapillary plate

Laser-Generated & Other Lab. X-Ray & EUV Sources, Optics, Apps., ed. G. A. Kyrala, J.-C. J. Gauthier, C. A. MacDonald, A. M. Khounsary, Proceedings of SPIE Vol. 5196 (SPIE, Bellingham, WA, 2004) · 0277-786X/04/$15 · doi: 10.1117/12.505433

1. INTRODUCTION

Monochromatic parallel x-ray beams are typically produced by a synchrotron in conjunction with single crystals and have been applied in high contrast micro-angiography[1] and x-ray phase imaging.[2-4] In order to produce quasi-monochromatic x-rays without using the synchrotron, we developed a transmission type molybdenum x-ray tube.[5] Subsequently, flash x-ray tubes are employed to primarily perform high speed radiographies with biomedical applications. In particular, plasma flash x-ray tubes are very useful to produce intense and sharp characteristic x-rays[6-11] such as lasers.

With recent advances in x-ray optics, several different x-ray lenses[12,13] have been developed, and a polycapillary plate[5,8,14] has been shown to be useful to realize a low-priced x-ray system and to perform parallel radiography. Therefore, we performed parallel radiography using a tungsten-target x-ray tube and an x-ray film because the film is conventional and is useful to obtain a high image resolution.

In biomedical radiography, because both the brightness and the contrast of radiograms can be controlled by a Computed Radiography (CR) system[15] utilizing imaging plates, the CR system is useful to perform quasi-monochromatic parallel radiography, regardless of whether the image resolution falls. Therefore, in conjunction with the CR, we have to measure the fundamental characteristics of the polycapillary radiography.

In this paper, we describe a quasi-monochromatic parallel radiography system utilizing a fine polycapillary plate with a hole diameter of 10 μm, a CR system, and a copper-target radiation tube in order to create a conventional x-ray system to be used instead of the synchrotron.

2. EXPERIMENTAL SETUP

Figure 1 shows the circuit diagram of the x-ray generator, which consists of a negative high-voltage power supply, a filament (hot cathode) power supply, and a copper-target x-ray tube. The negative high-voltage is applied to the cathode electrode, and the anode (target) is connected to the ground. In this experiment, the tube voltage was regulated from 12 to 22 kV, and the tube current was regulated by the filament temperature and ranged from 1.0 to 3.0 mA. The exposure time was controlled in order to obtain optimum x-ray intensity.

The experimental setup for performing parallel radiography is shown in Fig. 2. Quasi-monochromatic x-rays are produced using a 10 μm-thick copper filter, and these rays are formed into parallel beams by a polycapillary plate (Fig. 3). The polycapillary is J5022-16 (Hamamatsu Photonics Inc.), and the thickness and the hole diameter of the polycapillary are 1.0 mm and 10 μm, respectively. Radiography was performed by a CR system (Konica Regius 150) utilizing imaging plates.

The distance between the x-ray source and the polycapillary was 1.08 m, and the polycapillary plate was set on the aluminum plate. The distance between the polycapillary and imaging plates was regulated by the height of polymethyl methacrylate (PMMA) spacers of 30 mm in height. At a constant distance between the polycapillary and the imaging plate, the distance between the imaging plate and the chart was regulated by pipe-shaped brass spacers of 30 and 60 mm in height.

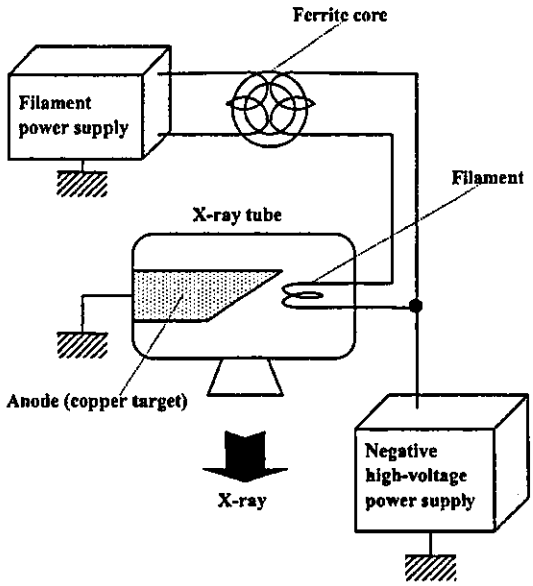

Figure 1: Circuit diagram of the x-ray generator.

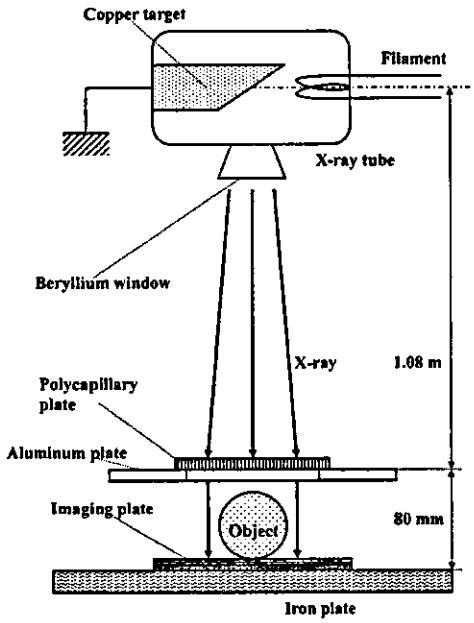

Figure 2: Experimental setup for parallel radiography utilizing a polycapillary plate and a CR system.

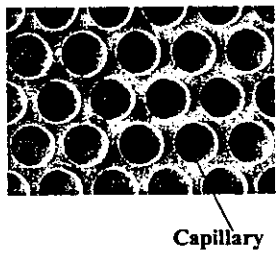

Figure 3: Polycapillary plate.

3. CHARACTERISTICS

3.1 Focal spot

In order to measure images of the x-ray source, we employed a pinhole camera with a hole diameter of 50 μm (Fig. 4). When the tube voltage was increased, the spot intensity increased, and spot dimensions increased slightly and had values of approximately 2.0×1.5 mm.

3.2 X-ray spectra

X-ray spectra from the copper-target tube were measured by a transmission-type spectrometer with a lithium fluoride curved crystal 0.5 mm in thickness (Fig. 5). The spectra were taken by the CR system with a wide dynamic range, and relative x-ray intensity was calculated from Dicom digital data. Figure 6 shows measured spectra from the

copper target. When the tube voltage was increased, the bremsstrahlung x-ray intensity increased, and the characteristic x-ray intensity of K_α and K_β lines also increased. Following insertion of the copper filter, the bremsstrahlung x-rays with energies higher than the K-absorption edge were absorbed effectively.

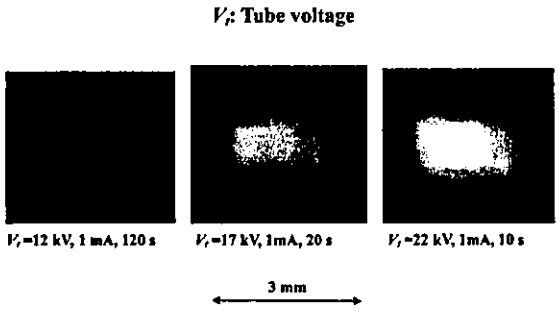

Figure 4: Images of the x-ray source measured by a 50 μm-diameter pinhole with changes in the tube voltage.

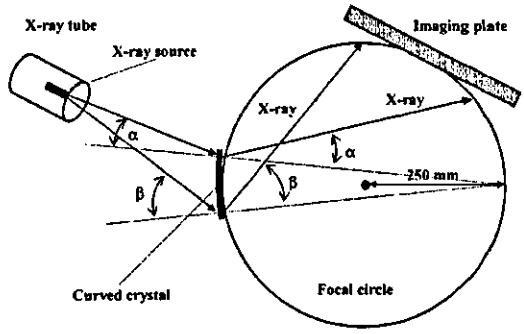

Figure 5: Transmission-type spectrometer with a lithium fluoride curved crystal and an imaging plate.

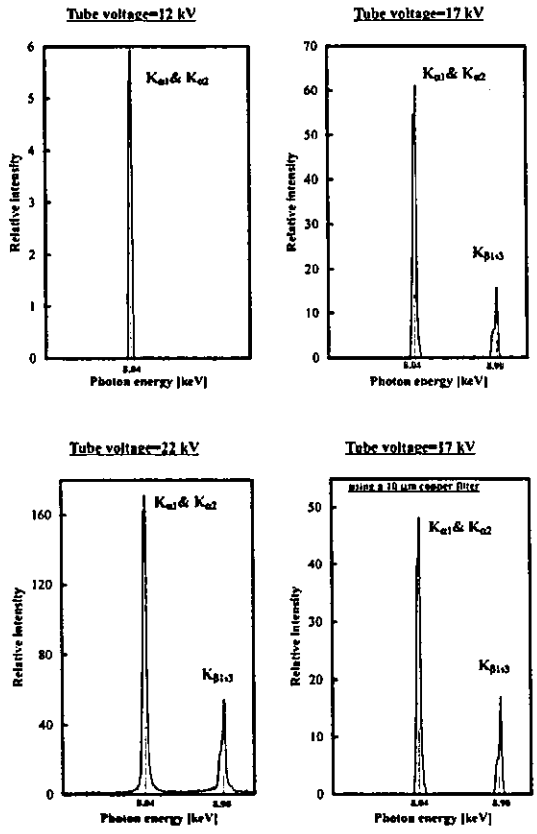

Figure 6: Measured x-ray spectra according to changes in the tube voltage.

4. RADIOGRAPHY

The quasi-monochromatic radiography was performed with a tube voltage of 17 kV using the filter. Figure 7 shows radiography for imaging a polycapillary plate, and the radiograms of the polycapillary are shown in Fig. 8. The center of the black spot in the polycapillary radiogram was mainly imaged by direct transmission beams through capillary holes. As shown in this figure, the spot dimensions increased slightly according to decreases in the PMMA spacer height.

Figure 9 shows the parallel radiography for imaging a test chart, and the polycapillary was set on the aluminum plate. In this radiography, when the spacer height was increased, the image resolution hardly varied, and the image dimensions decreased slightly (Fig. 10). Next, when the height of the brass spacer was decreased, the image resolution hardly varied, and the dimensions again decreased slightly (Figs. 11 and 12).

Figures 13 and 14 show radiography and the radiogram of tungsten wires on a PMMA spacer, respectively. Although the image contrast increased with increases in the wire diameter, a 50 μm-diameter wire could be observed. An angiography of a rabbit heart is shown in Fig. 15; iodine-based microspheres of 20 μm diameter were used, and fine blood vessels of about 50 μm were visible (Fig. 16).

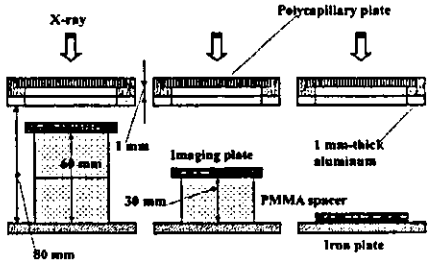

Figure 7: Radiography for imaging a polycapillary plate according to changes in the distance between the polycapillary and imaging plates.

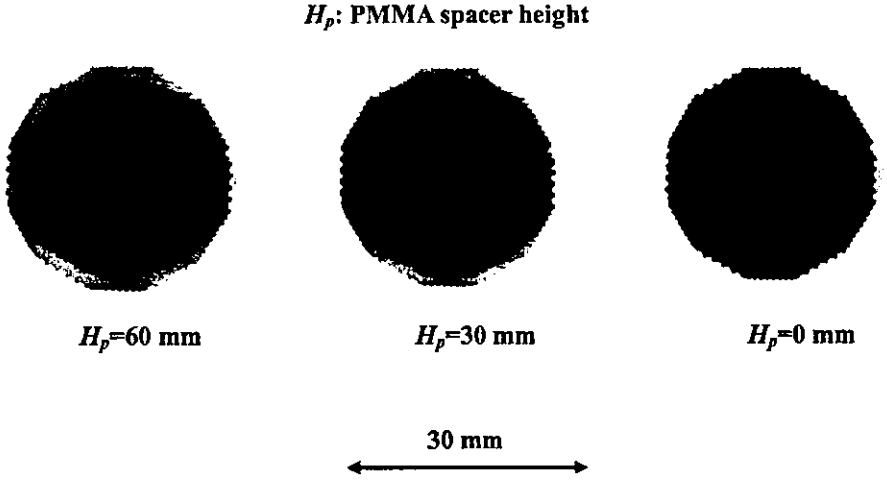

Figure 8: Radiograms of a polycapillary plate according to changes in the PMMA height.

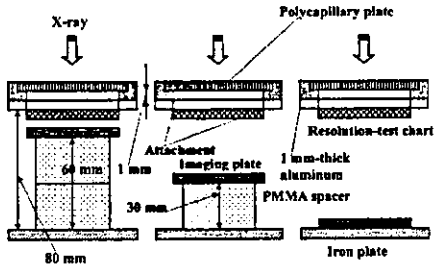

Figure 9: Radiography for imaging a test chart using a polycapillary plate according to the PMMA height.

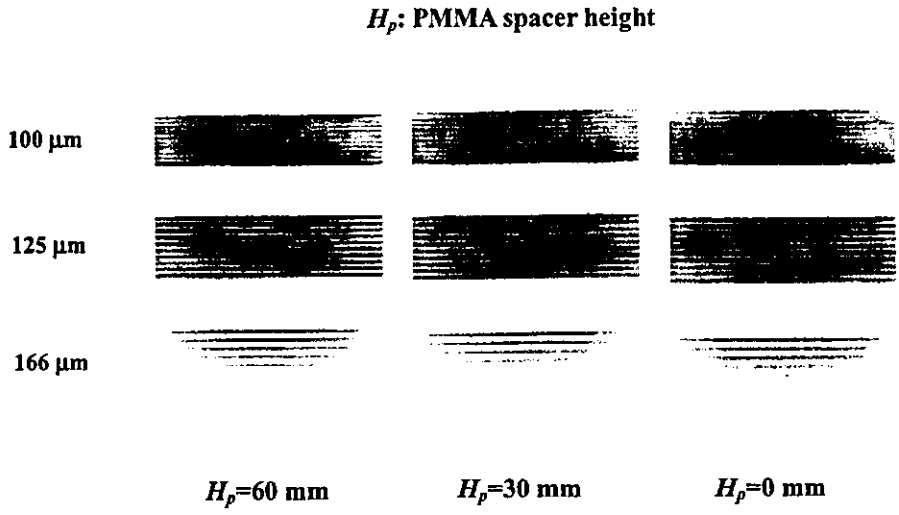

Figure 10: Radiograms of a test chart using a polycapillary plate according to the PMMA height.

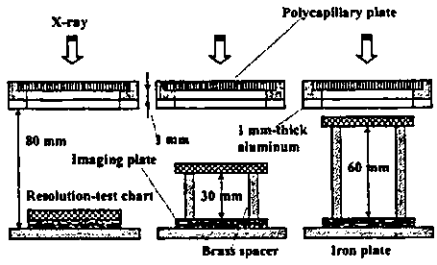

Figure 11: Radiography for imaging a test chart using a polycapillary plate according to the brass spacer height.

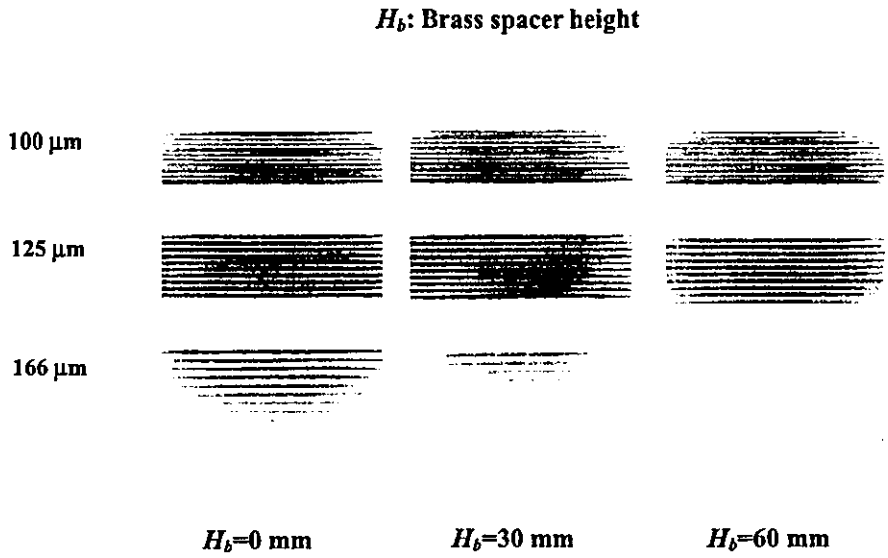

Figure 12: Radiograms of a test chart using the polycapillary according to the brass spacer height.

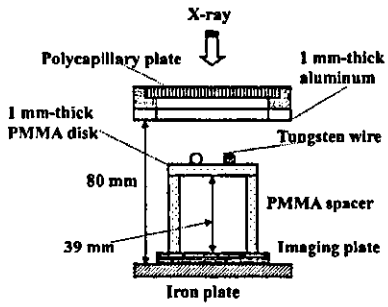

Figure 13: Radiography for imaging tungsten wires using the polycapillary.

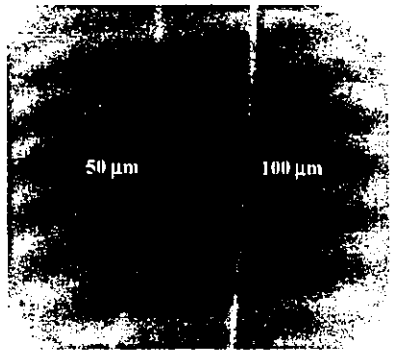

Figure 14: Radiograms of tungsten wires on a PMMA spacer.

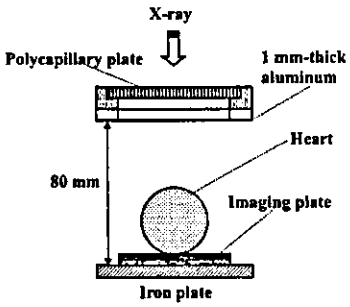

Figure 15: Parallel angiography of a heart extracted from a rabbit using iodine-based microspheres.

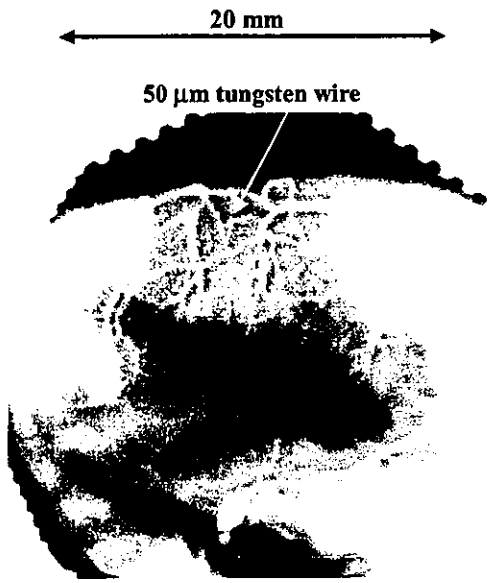

Figure 16: Angiogram of the heart using the polycapillary.

5. DISCUSSION

In this research, we performed parallel radiography achieved with a polycapillary plate in conjunction with quasi-monochromatic x-rays, and obtained slightly higher image resolutions as compared with those obtained without using the plate. Currently, the image resolution of the polycapillary is primarily determined by the diameter of the capillary hole and the thickness, and is improved with decreases in the diameter and increases in the thickness. In cases where the CR system is employed, although the resolution of the CR system is primarily determined by the minimum sampling pitch of 87.5 μm, we could observe 50 μm tungsten wires easily.

The photon energies of the characteristic x-rays are determined by the target element, and the capillary thickness should be increased according to increases in the photon energy because the transmission intensity through capillary glass increases. Subsequently, in order to increase the parallelity for phase imaging, single crystals should be employed after passing through the polycapillary.

Because it is possible to increase the irradiation field by increasing the distance between the x-ray source and the polycapillary, this system can be applied to image a wide variety of objects in various fields, including medical radiography.

ACKNOWLEDGMENTS

This work was supported by Grants-in-Aid for Scientific Research (12670902, 13470154, and 13877114) and Advanced Medical Scientific Research from MECSST, Grants from Keiryo Research Foundation, JST (Test of Fostering Potential), NEDO, and MHLW (HLSRG, RAMT-nano-001, RHGTEFB-genome-005, and RGCD13C-1).

REFERENCES

1. H. Mori, K. Hyodo, E. Tanaka, M.U. Mohammed, A. Yamakawa, Y. Shinozaki, H. Nakazawa, Y. Tanaka, T. Sekka, Y. Iwata, S. Honda, K. Umetani, H. Ueki, T. Yokoyama, K. Tanioka, M. Kubota, H. Hosaka, N. Ishizawa and M. Ando, "Small-vessel radiography in situ with monochromatic synchrotoron radiation," *Radiology*, **201**, pp. 173-177, 1996.

2. T.J. Davis, D. Gao, T.E. Gureyev, A.W. Stevenson and S.W. Wilkims, "Phase-contrast imagimg of weakly absorbing materials using hard x-rays," *Nature*, **373**, pp. 595-597, 1995.

3. A. Momose, T. Takeda, Y. Itai and K. Hirano, "Phase-contrast x-ray computed tomography for observing biological soft tissues," *Nature Medicine*, **2(4)**, pp. 473-475, 1996.

4. A. Ishisaka, H. Ohara and C. Honda, "A new method of analyzing edge effect in phase contrast imaging with incoherent x-rays," *Opt. Rev*, **7**, pp. 566-572, 2000.

5. E. Sato, M. Komatsu, Y. Hayasi, E. Tanaka, H. Mori, T. Kawai, T. Usuki, K. Sato, T. Ichimaru, K. Takayama and H. Ido, "Quasi-monochromatic parallel radiography achieved with a plane-focus x-ray tube," *SPIE*, **4786**, pp. 151-161. 2002.

6. E. Sato, Y. Hayasi, H. Mori, E. Tanaka, K. Takayama, H. Ido, K. Sakamaki and Y. Tamakawa, "Quasi-monochromatic x-ray production from the cerium target," *SPIE*, **4142**, pp. 17-28, 2000.

7. E. Sato, Y. Suzuki, Y. Hayashi, E. Tanaka, H. Mori, T. Kawai, K. Takayama, H. Ido and Y. Tamakawa, "High-intensity quasi-monochromatic x-ray irradiation from the linear plasma target," *SPIE*, **4505**, pp. 154-164, 2001.

8. E. Sato, Y. Hayashi, E. Tanaka, H. Mori, T. Kawai, H. Obara, T. Ichimaru, K. Takayama, H. Ido, T. Usuki, K. Sato and Y. Tamakawa, "Polycapillary radiography using a quasi-x-ray laser generator," *SPIE*, **4508**, pp. 176-187, 2001.

9. E. Sato, Y. Hayasi, E. Tanaka, H. Mori, T. Kawai, T. Usuki, K. Sato, H. Obara, T. Ichimaru, K. Takayama, H. Ido and Y. Tamakawa, "Quasi-monochromatic radiography using a high-intensity quasi-x-ray laser generator," *SPIE*, **4682**, pp. 538-548 2002.

10. E. Sato, Y. Hayasi, E. Tanaka, H. Mori, T. Kawai, K. Takayama and H. Ido, "Irradiation of intense characteristic x-rays from weakly ionized linear plasma," *Proc 3rd Korea-Japan Joint Meeting on Medical Physics, Gyeongju*, pp. 396-399, 2002.

11. E. Sato, Y. Hayasi, R. Germer, E. Tanaka, H. Mori, T. Kawai, H. Obara, T. Ichimaru, K. Takayama and H. Ido, "Intense characteristic x-ray irradiation from weakly ionized linear plasma and applications," *Jpn. J. Med. Imag. Inform. Sci.*, **20**, pp. 148-155. 2003.

12. Q.F. Xiao and S.V. Poturaef, "Polycapillary-based x-ray optics," *Nucl. Instr. Meth. Phys. Res. A*, **347**, pp. 376-383, 1994.

13. A.A. Bzhanmikov, N. Langhoff, J. Schmalz, R. Wedell, V.L. Beloglazov and N.F. Lebedev, "Polycapillary conic collimator for micro-XRF," *SPIE*, **3444**, pp. 430-435, 1998.

14. E. Sato, H. Toriyabe, Y. Hayasi, E. Tanaka, H. Mori, T. Kawai, T. Usuki, K. Sato, H. Obara, T. Ichimaru, K. Takayama, H. Ido and Y. Tamakawa,"Fundamental study on parallel beam radiography using a polycapillary plate," *SPIE*, **4682**, pp. 298-310, 2002.

15. E. Sato , K. Sato and Y. Tamakawa, "Film-less computed radiography system for high-speed Imaging," *Ann. Rep. Iwate Med. Univ. Sch. Lib. Arts and Sci.*, **35**, pp. 13-23, 2000.

Effects of Adrenomedullin Inhalation on Hemodynamics and Exercise Capacity in Patients With Idiopathic Pulmonary Arterial Hypertension

Noritoshi Nagaya, MD; Shingo Kyotani, MD; Masaaki Uematsu, MD; Kazuyuki Ueno, PhD; Hideo Oya, MD; Norifumi Nakanishi, MD; Mikiyasu Shirai, MD; Hidezo Mori, MD; Kunio Miyatake, MD; Kenji Kangawa, PhD

Background—Adrenomedullin (AM) is a potent pulmonary vasodilator peptide. However, whether intratracheal delivery of aerosolized AM has beneficial effects in patients with idiopathic pulmonary arterial hypertension remains unknown. Accordingly, we investigated the effects of AM inhalation on pulmonary hemodynamics and exercise capacity in patients with idiopathic pulmonary arterial hypertension.

Methods and Results—Acute hemodynamic responses to inhalation of aerosolized AM (10 μg/kg body wt) were examined in 11 patients with idiopathic pulmonary arterial hypertension during cardiac catheterization. Cardiopulmonary exercise testing was performed immediately after inhalation of aerosolized AM or placebo. The work rate was increased by 15 W/min until the symptom-limited maximum, with breath-by-breath gas analysis. Inhalation of AM produced a 13% decrease in mean pulmonary arterial pressure (54±3 to 47±3 mm Hg, $P<0.05$) and a 22% decrease in pulmonary vascular resistance (12.6±1.5 to 9.8±1.3 Wood units, $P<0.05$). However, neither systemic arterial pressure nor heart rate was altered. Inhalation of AM significantly increased peak oxygen consumption during exercise (peak $\dot{V}O_2$, 14.6±0.6 to 15.7±0.6 mL · kg^{-1} · min^{-1}, $P<0.05$) and the ratio of change in oxygen uptake to that in work rate ($\Delta\dot{V}O_2/\Delta W$ ratio, 6.3±0.4 to 7.0±0.5 mL · min^{-1} · W^{-1}, $P<0.05$). These parameters remained unchanged during placebo inhalation.

Conclusions—Inhalation of AM may have beneficial effects on pulmonary hemodynamics and exercise capacity in patients with idiopathic pulmonary arterial hypertension. (***Circulation.*** **2004;109:351-356.)**

Key Words: peptides ■ hypertension, pulmonary ■ respiration ■ exercise ■ hemodynamics

Idiopathic pulmonary arterial hypertension is a rare but life-threatening disease characterized by progressive pulmonary hypertension, ultimately producing right heart failure and death.[1,2] Although a variety of vasodilators have been proposed as potential therapy for this disease over the past 30 years,[3–7] some patients ultimately require heart-lung or lung transplantation.[8,9] Thus, a novel therapeutic strategy is desirable.

Adrenomedullin (AM) is a potent, long-lasting vasodilator peptide that was originally isolated from human pheochromocytoma.[10] Immunoreactive AM has subsequently been detected in plasma and a variety of tissues, including blood vessels and lungs.[11,12] It has been reported that there are abundant binding sites for AM in the lungs.[13] We have shown that the plasma AM level increases in proportion to the severity of pulmonary hypertension and that circulating AM is partially metabolized in the lungs.[14,15] Interestingly, AM has been shown to inhibit the migration and proliferation of vascular smooth muscle cells.[16,17] These findings suggest that AM plays an important role in the regulation of pulmonary vascular tone and vascular remodeling. In fact, we have shown that short-term intravenous infusion of AM significantly decreases pulmonary vascular resistance in patients with congestive heart failure[18] or pulmonary arterial hypertension.[19] Unfortunately, however, intravenously administered AM induced systemic hypotension in such patients because of nonselective vasodilation in the pulmonary and systemic vascular beds.

More recently, inhalation of aerosolized prostacyclin and its analogue iloprost has been shown to cause pulmonary vasodilation without systemic hypotension in patients with idiopathic pulmonary arterial hypertension.[20,21] In addition, inhalant application of vasodilators does not impair gas exchange because the ventilation-matched deposition of drug

Received February 3, 2003; de novo received July 28, 2003; revision received October 15, 2003; accepted October 19, 2003

From the Department of Internal Medicine, National Cardiovascular Center, Osaka (N. Nagaya, S.K., H.O., N. Nakanishi, K.M.); the Cardiovascular Division, Kansai Rosai Hospital, Hyogo (M.U.); the Department of Pharmacy, National Cardiovascular Center, Osaka (K.U.); the Department of Cardiac Physiology, National Cardiovascular Center Research Institute, Osaka (M.S., H.M.); and the Department of Biochemistry, National Cardiovascular Center Research Institute, Osaka (K.K.), Japan

Correspondence to Noritoshi Nagaya, MD, Department of Internal Medicine, National Cardiovascular Center, 5-7-1 Fujishirodai, Suita, Osaka 565-8565, Japan. E-mail nagayann@hsp.ncvc.go.jp

Circulation **is available at http://www.circulationaha.org** **DOI: 10.1161/01.CIR.0000109493.05849.14**

TABLE 1. Baseline Characteristics of Patients With Idiopathic Pulmonary Arterial Hypertension

Demographics	
Age, y	39±3
Male/female, n	2/9
NYHA functional class, n	
III	10
IV	1
Baseline hemodynamics	
MPAP, mm Hg	54±3
CI, L·min^{-1}·m^{-2}	2.4±0.1
PVR, Wood units	12.6±1.5
RAP, mm Hg	7±1
PCWP, mm Hg	7±1
Pulmonary function	
Sa_{O_2}, %	94±3
Svo_2, %	63±4
FVC, % predicted	86 4
FEV_1, % predicted	75±1
6-Minute walk test, m	355±35
Medication use, n	
Anticoagulant agents	10
Diuretics	9
Digitalis	7
Oral prostacyclin analogue	6
Calcium antagonists	2

NYHA indicates New York Heart Association; MPAP, mean pulmonary arterial pressure; CI, cardiac index; PVR, pulmonary vascular resistance; RAP, mean right atrial pressure; PCWP, pulmonary capillary wedge pressure; Sa_{O_2}, arterial oxygen pressure; Svo_2, mixed venous oxygen saturation; FVC, forced vital capacity; and FEV_1, forced expiratory volume in 1 second. Data are mean±SEM.

in the alveoli causes pulmonary vasodilation matched to ventilated areas.[20] In clinical settings, inhalation therapy may be more simple, noninvasive, and comfortable than continuous intravenous infusion therapy. Thus, the purpose of the present study was to investigate the effects of AM inhalation on hemodynamics and exercise capacity in patients with idiopathic pulmonary arterial hypertension.

Methods

Study Subjects

Eleven patients with idiopathic pulmonary arterial hypertension (9 women and 2 men; age, 39±3 years) were included in this study. Idiopathic pulmonary arterial hypertension was defined as pulmonary hypertension unexplained by any secondary cause, on the basis of the criteria of the National Institutes of Health registry.[1] Ten patients were classified as New York Heart Association (NYHA) functional class III and 1 as class IV (Table 1). Two of the 11 patients (18%) were acute responders who showed a significant decrease in mean pulmonary arterial pressure of ≥20% with a decrease in mean pulmonary arterial pressure to <35 mm Hg and no change or an increase in cardiac index during short-term infusion of epoprostenol. Long-term medication, including anticoagulant agents, digitalis, and diuretics, was kept constant. Vasodilator agents, such as oral prostacyclin analogue and calcium antagonists, were stopped ≥12 hours before the study procedure was begun. The ethics committee of the National Cardiovascular Center approved the study, and all patients gave written informed consent.

Preparation of Human AM

Human AM was dissolved in saline with 4% D-mannitol and sterilized by passage through a 0.22-μm filter (Millipore Co). At the time of dispensing, randomly selected vials were submitted for sterility and pyrogen testing. The chemical nature and content of the human AM in vials were verified by high-performance liquid chromatography and radioimmunoassay. All vials were stored frozen at −80°C from the time of dispensing until the time of preparation for administration.

Hemodynamic Studies

Acute hemodynamic responses to AM inhalation were assessed in all patients while they were in a stable condition during hospitalization. Hemodynamic variables, including pulmonary arterial pressure, right atrial pressure, pulmonary capillary wedge pressure, and cardiac output (in triplicate), were determined with a thermodilution catheter (TOO21H-7.5F, Baxter Co).[22] A 22-gauge cannula was inserted into a radial artery for hemodynamic measurements and blood sampling. After an equilibration period of 30 minutes, baseline hemodynamics were measured. Then, AM (10 μg/kg body wt) was inhaled as an aerosol with a jet nebulizer (Porta-Nebu, MEDIC-AID) for 15 minutes, which resulted in a cumulative dose of 400 to 600 μg AM. Hemodynamic parameters were measured at 15-minute intervals starting 15 minutes before AM inhalation until 60 minutes after inhalation. Blood samples for AM measurement were taken at 15-minute intervals from 15 minutes before inhalation until 60 minutes after the end of inhalation.

Cardiopulmonary Exercise Testing

The effects of AM inhalation on exercise capacity were examined in 10 of 11 patients; 1 patient with NYHA class IV underwent the 6-minute walk test according to decision of attending physicians. Cardiopulmonary exercise testing was performed immediately after inhalation of aerosolized AM (10 μg/kg body wt) or saline in a double-blind, randomized, crossover design. This study was performed on 2 separate days, 1 week apart. The first cardiopulmonary exercise testing was performed within 10 days after the cardiac catheterization. The patients performed exercise seated on a cycle ergometer. They first pedaled at 55 rpm without any added load for 1 minute. The work rate was then increased by 15 W/min up to the symptom-limited maximum. Breath-by-breath gas analysis was performed with an AE280 (Minato Medical Science) connected to a personal computer running analyzing software.[23] The ratio of change in oxygen uptake to that in work rate ($\Delta\dot{V}O_2/\Delta W$ ratio) was calculated as the slope of oxygen consumption per unit workload from 1 minute after the start of load addition until 85% maximal $\dot{V}O_2$. Exercise capacity was evaluated by peak oxygen consumption (peak $\dot{V}O_2$), which was defined as the value of averaged data during the final 15 seconds of exercise. Ventilatory efficiency during exercise was represented by the $\dot{V}E$-$\dot{V}CO_2$ slope, which was determined as the linear regression slope of $\dot{V}E$ and $\dot{V}CO_2$ from the start of exercise until the RC point (the time until which ventilation is stimulated by CO_2 output and end-tidal CO_2 tension begins to decrease).

Measurement of Plasma AM, cAMP, and cGMP

Blood samples were immediately transferred into chilled glass tubes containing disodium EDTA (1 mg/mL) and aprotinin (500 U/mL) and centrifuged immediately at 4°C, and the plasma was frozen and stored at −80°C until assayed. Plasma AM level was measured by a specific immunoradiometric assay kit (Shionogi Pharmaceutical Co Ltd).[24] Plasma cAMP and cGMP were determined with radioimmunoassay kits (cAMP assay kit, cGMP assay kit, Yamasa Shoyu).[18]

Statistical Analysis

All data were expressed as mean±SEM unless otherwise indicated. Changes in hemodynamic and hormonal parameters by AM inhalation were analyzed by 1-way ANOVA for repeated measures,

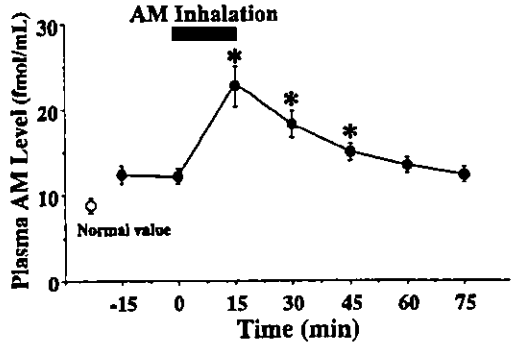

Figure 1. Changes in plasma AM level by inhalation of aerosolized AM in patients with idiopathic pulmonary arterial hypertension. Normal value indicates plasma AM level derived from 15 age-matched healthy subjects. Data are mean ± SEM. *$P<0.05$ vs value at time 0.

followed by Newman-Keuls test. Comparisons of exercise parameters between the 2 groups were analyzed with paired Student's t test. A probability value of $P<0.05$ was considered statistically significant.

Results

All patients tolerated this study protocol. One patient developed a headache, and another patient had mild arterial hypoxemia during AM inhalation. None of them experienced other adverse effects, such as systemic hypotension, infection, or arrhythmia.

Plasma AM Level After Inhalation

Baseline plasma AM level in patients with idiopathic pulmonary arterial hypertension was significantly higher than the normal value, which was determined from pooled data of 15 age-matched healthy subjects (11.9±0.8 versus 9.3±0.1 fmol/mL, $P<0.05$). Inhalation of AM significantly increased the plasma AM level to 22.9±2.1 fmol/mL immediately after inhalation (Figure 1). The half-life of plasma AM after inhalation was approximately 20 minutes, and the elevation of AM lasted for >45 minutes. Plasma cAMP level increased significantly 30 minutes after the initiation of AM inhalation (10.8±0.7 to 12.0±0.6 pmol/mL, $P<0.05$), although plasma cGMP level was not significantly altered (6.5±1.0 to 6.8±1.0 pmol/mL, P=NS).

Hemodynamic Effects of AM Inhalation

Inhalation of AM significantly decreased mean pulmonary arterial pressure in patients with idiopathic pulmonary arterial hypertension (54±3 to 47±3 mm Hg, $P<0.05$) without a significant decrease in mean arterial pressure (85±4 to 83±4 mm Hg, P=NS) (Figure 2). AM inhalation slightly but significantly increased cardiac index by 12% (2.4±0.1 to 2.7±0.2 L · min^{-1} · m^{-2}, $P<0.05$). Thus, AM inhalation resulted in a 22% decrease in pulmonary vascular resistance (12.6±1.5 to 9.8±1.3 Wood units, $P<0.05$) (Figure 3). Inhaled AM did not significantly alter systemic vascular resistance. The ratio of pulmonary vascular resistance to systemic vascular resistance was decreased significantly at the end of inhalation (0.63±0.08 to 0.55±0.07, $P<0.05$). These hemodynamic effects of AM lasted for >45 minutes.

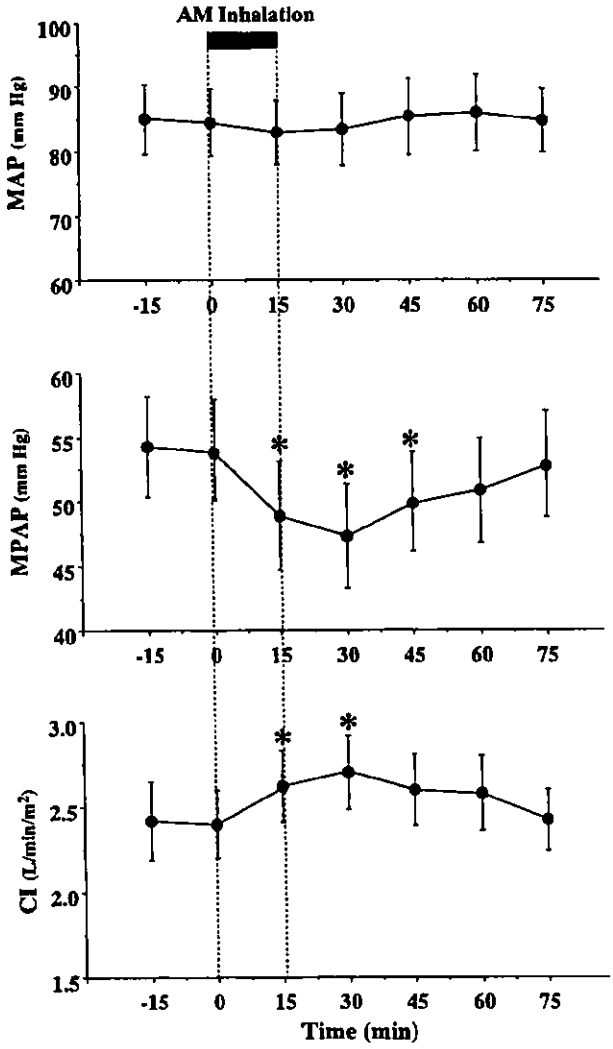

Figure 2. Changes in mean arterial pressure (MAP), mean pulmonary arterial pressure (MPAP), and cardiac index (CI) by inhalation of aerosolized AM in patients with idiopathic pulmonary arterial hypertension. Data are mean ± SEM. *$P<0.05$ vs value at time 0.

No significant change in heart rate, pulmonary capillary wedge pressure, or right atrial pressure was observed. There was no significant change in arterial oxygen saturation (94±3% to 93±3%).

Effects of AM Inhalation on Exercise Capacity and Ventilatory Efficiency

As the limiting symptom at the end of exercise, 6 patients reported muscle weakness and 4 reported dyspnea. There was no difference in these symptoms when exercise testing was performed with or without inhalation of AM. Inhalation of AM altered neither heart rate nor blood pressure either at rest or at peak exercise (Table 2). Inhalation of AM significantly increased peak workload (86±5 to 93±6 W, $P<0.05$) (Table 2). AM also significantly increased peak $\dot{V}o_2$ (14.6±0.6 to 15.7±0.6 mL · kg^{-1} · min^{-1}, $P<0.05$) (Figure 4). Inhalation of AM significantly increased $\Delta\dot{V}o_2/\Delta W$ ratio (6.3±0.4 to

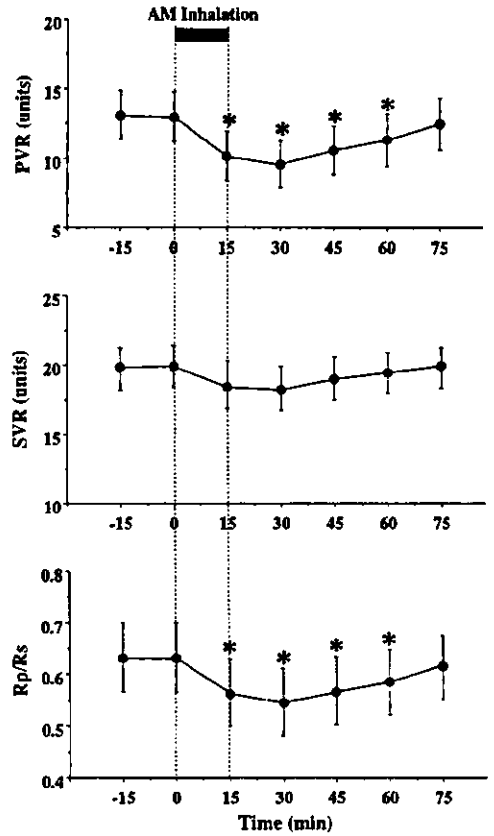

Figure 3. Changes in pulmonary vascular resistance (PVR), systemic vascular resistance (SVR), and ratio of pulmonary vascular resistance to systemic vascular resistance (Rp/Rs) by inhalation of aerosolized AM in patients with idiopathic pulmonary arterial hypertension. Data are mean ± SEM. *$P<0.05$ vs value at time 0.

7.0±0.5 mL · min^{-1} · W^{-1}, $P<0.05$). AM did not significantly alter the $\dot{V}_E$-$\dot{V}_{CO_2}$ slope (Table 2). No significant changes in arterial oxygen saturation were observed either at rest or at peak exercise. In 1 patient with NYHA class IV who did not undergo cardiopulmonary exercise testing, the distance walked in 6 minutes increased from 150 to 180 m by inhalation of AM.

Discussion

In the present study, we demonstrated that inhalation of AM improved hemodynamics with pulmonary selectivity and exercise capacity in patients with idiopathic pulmonary arterial hypertension.

AM is one of the most potent endogenous vasodilators in the pulmonary vascular bed.[25-27] The vasodilatory effect is mediated by cAMP-dependent and nitric oxide dependent mechanisms.[28,29] Endogenous AM production is enhanced in a variety of cardiovascular diseases through a compensatory mechanism.[14,30] Nonetheless, additional supplementation of AM has beneficial effects in these diseases.[18,19] These results suggest that endogenous AM level is not sufficient to improve deteriorated conditions despite the increased AM production. Interestingly, Champion et al[31] have shown that intratracheal gene transfer of calcitonin gene related peptide, a member of the same peptide family as AM, to bronchial

TABLE 2. Changes in Exercise Parameters by Inhalation of AM or Placebo

Variables	Placebo	AM	*P*
Peak workload, W	86±5	93±6	<0.05
HR, bpm			
Rest	75±5	75±3	NS
Peak	144±6	148±6	NS
MAP, mm Hg			
Rest	85 3	87 5	NS
Peak	108±5	110±6	NS
Peak Borg score (D/L)	17/18	18/18	NS
Peak $\dot{V}o_2$, mL · kg^{-1} · min^{-1}	14.6±0.6	15.7±0.6	<0.05
$\Delta\dot{V}o_2/\Delta W$ ratio, mL · min^{-1} · W^{-1}	6.3±0.4	7.0±0.5	<0.05
$\dot{V}_E$-$\dot{V}co_2$ slope	37±2	36±2	NS
Sa_{O_2}, %			
Rest	97±1	97±1	NS
Peak	95±1	95±1	NS

HR indicates heart rate; MAP, mean arterial pressure; Peak Borg score (D/L), Borg score at peak exercise (dyspnea/leg fatigue); Peak $\dot{V}o_2$, peak oxygen consumption; $\Delta\dot{V}o_2/\Delta W$ ratio, $\dot{V}o_2$ increase per unit workload; $\dot{V}_E$-$\dot{V}co_2$ slope, slope of regression line of relation between $\dot{V}_E$ and $\dot{V}co_2$; and Sa_{O_2}, arterial oxygen saturation. Data are mean ± SEM.

epithelial cells attenuates chronic hypoxia-induced pulmonary hypertension in the mouse. These results raise the possibility that intratracheal delivery of a vasodilator peptide may be sufficient to alter pulmonary vascular function. In fact, in the present study, inhalation of AM significantly decreased pulmonary vascular resistance, whereas it did not alter systemic arterial pressure or systemic vascular resistance. The ratio of pulmonary vascular resistance to systemic vascular resistance was reduced significantly by AM inhalation. These results suggest that inhaled AM improves hemodynamics with pulmonary selectivity. This is consistent with earlier findings that inhaled prostacyclin or its analogue iloprost acts transepithelially with pulmonary selectivity and improves pulmonary hypertension.[20,21] Inhalation of AM slightly but significantly increased cardiac index in patients with idiopathic pulmonary arterial hypertension. Considering the strong vasodilator activity of AM in the pulmonary vasculature, the significant decrease in cardiac afterload may be responsible for increased cardiac index with

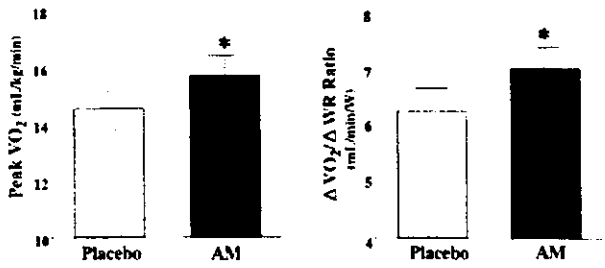

Figure 4. Changes in peak oxygen consumption (peak $\dot{V}o_2$) and ratio of change in oxygen uptake to that in work rate ($\Delta\dot{V}o_2/\Delta W$ ratio) by inhalation of aerosolized AM or placebo in patients with idiopathic pulmonary arterial hypertension. Data are mean ± SEM. *$P<0.05$ vs placebo.